

## High-density, uniform InSb/GaSb quantum dots emitting in the midinfrared region

V. Tasco, N. Deguffroy, A. N. Baranov, and E. Tournié<sup>a)</sup>

*Intitut d'Electronique du Sud, Université Montpellier 2-CNRS, UMR 5214, Place Eugène Bataillon, F-34095 Montpellier cedex 5, France*

B. Satpati and A. Trampert

*Paul-Drude-Institut für Festkörperelektronik, Hausvogteiplatz 5-7, D-10117 Berlin, Germany*

M. S. Dunaevskii and A. Titkov

*Ioffe-Physico-Technical Institute, St. Petersburg, Russia 194021*

(Received 20 October 2006; accepted 26 November 2006; published online 29 December 2006)

The authors have developed a multistep molecular-beam epitaxy growth technique which allows them to grow InSb quantum dots with high structural perfection and high density. This technique consists in the deposition at a very low temperature followed by a properly designed annealing step. Fully strained InSb/GaSb quantum dots with a density exceeding  $7 \times 10^{10} \text{ cm}^{-2}$  and lateral sizes in the 20–30 nm range have been obtained. Narrow photoluminescence emission is obtained around  $3.5 \mu\text{m}$  up to room temperature. © 2006 American Institute of Physics. [DOI: 10.1063/1.2425041]

InSb is a very interesting compound for both electronics and optoelectronics applications. It has a very small effective electron mass, a very high electron mobility, and a large  $g$  factor, properties which are desirable for high speed, low power transistors, spintronic, and quantum information devices.<sup>1</sup> In addition, its small band gap makes it attractive as active medium for light emitting diodes and lasers operating in the midinfrared region, in particular, in the 3–5  $\mu\text{m}$  band-II region where several technological applications (such as gas analysis, free space communication, laser assisted surgery, or imaging) find room. InSb/AlInSb quantum well light emitting diodes have recently shown efficient emission in this region at low temperature,<sup>1</sup> but the Auger effect strongly affects such kind of devices, limiting their performances at high temperature. Another appealing approach is the use of InSb quantum dots (QDs) as active medium for light emitting devices. One then expects both an emission in the 3–5  $\mu\text{m}$  region and the improvement of device performances, due to low dimensional properties of semiconductor QDs.<sup>2</sup>

However, despite the potential advantages of this QD material system, only few reports are available in the literature, in marked contrast to the InAs/GaAs case-study materials. The growth of InSb QDs has been investigated, both by molecular beam epitaxy (MBE) and metal organic vapor phase epitaxy (MOVPE), on different substrates: GaAs,<sup>3–5</sup> GaSb,<sup>4,6,7</sup> InP,<sup>8</sup> and InAs.<sup>4,5,9</sup> In particular, if InSb/GaSb QDs are reported<sup>6,7</sup> to follow the Stranski-Krastanow growth mode, all groups working in the field have obtained QD densities in the  $10^9 \text{ dot/cm}^2$  range with typically large dot lateral size (50–100 nm). These nanostructures are said to exhibit photoluminescence (PL) emission only at low temperature and around 0.75 eV. Similar densities and sizes have been reported for InSb/InAs QDs grown by MBE (Ref. 5) while Ivanov *et al.*<sup>9</sup> obtained InSb/InAs submonolayer insertions by shortly exposing the InAs growth surface to an  $\text{Sb}_4$  flux. They report a density of  $10^{12} \text{ cm}^{-2}$  of extremely small inser-

tions (2.5 nm as lateral size).<sup>9</sup> Both groups observed PL between 3 and 4  $\mu\text{m}$  at 10 K,<sup>5,9</sup> while the submonolayer insertions emitted up to room temperature.<sup>10</sup> These emissions probably arise from type-II transitions. Shusterman *et al.*<sup>4</sup> have shown the formation of InSb QDs on various substrates by droplet heteroepitaxy during MOVPE. They obtained PL emission around 4  $\mu\text{m}$  at 10 K from InSb/GaAs QDs. All QDs, however, contain extended defects.<sup>4</sup> To summarize the published data, the growth of high quality InSb QDs, especially on GaSb, has proven impossible up to now whatever the epitaxial technique. This arises from the comparatively weak In–Sb binding energy which, in turn, results in a long migration length of In adatoms on an Sb-terminated surface.<sup>5,11</sup> This is confirmed by the fact that some improvement may be obtained when nucleating InSb QDs on an As-terminated surface.<sup>4,9,12</sup>

In this work, we show that high density, uniform, fully strained, InSb/GaSb QDs can be grown by means of a particular MBE technique, consisting of a deposition at an extremely low temperature followed by a properly designed annealing step.

The samples have been grown on GaSb(100) substrates by solid source MBE. Each sample contains either one plan of uncapped InSb QDs or one plan of InSb QDs inserted in the center of a GaSb barrier layer, itself confined on both sides by 100 nm thick AlGa(As)Sb lattice-matched claddings. *In situ* reflection high-energy electron diffraction (RHEED) has been used for monitoring the sample surface evolution. The surface morphology and structural properties of the as-grown samples have been investigated by atomic force microscopy (AFM) and transmission electron microscopy (TEM). PL measurements were performed at room temperature and at liquid nitrogen temperature. A semiconductor diode laser operating at 650 nm was used for optical pumping. The PL spectra were recorded using a Fourier transform infrared spectrometer equipped with a liquid-nitrogen-cooled InSb detector.

During the MBE growth of InSb QDs on GaSb at a substrate temperature around 450 °C we observe a Stranski-Krastanow growth mode with a two dimensional to three

<sup>a)</sup>Electronic mail: etournie@univ-montp2.fr

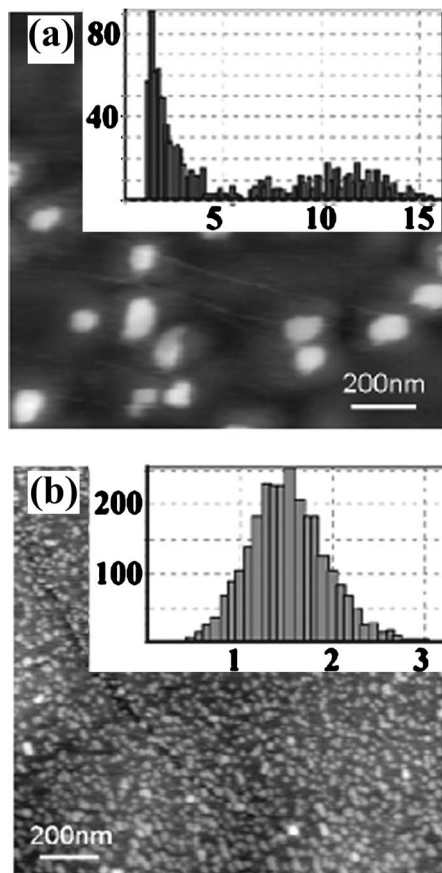


FIG. 1. AFM scan (size  $1 \times 1 \mu\text{m}^2$ ) on 2.6 ML of InSb deposited by the usual growth at  $450^\circ\text{C}$  (a) and deposited following the two step procedure (b). The insets are the related histograms for the height expressed in nm.

dimensional transition occurring after about 1.7 ML of InSb coverage. We show in Fig. 1(a) an AFM scan taken from 2.6 ML of InSb deposited at  $450^\circ\text{C}$  with a growth rate of  $0.33 \text{ ML/s}$ . The QD density is  $4 \times 10^9 \text{ dot/cm}^2$  with typical diameters of about 40–80 nm and heights of about 10–15 nm. Further, the InSb QDs exhibit a bimodal distribution, as shown by the size histogram in the inset of Fig. 1(a). Finally, plan-view as well as cross-section TEM reveal that all QDs are plastically relaxed.<sup>13</sup> Such results are in perfect agreement with previously published data.<sup>6,7</sup>

In order to increase the density of nucleation centers, and thus the QD density, the In-adatom migration length should be reduced. Typical MBE growth parameters which can affect the kinetics of the system are the growth temperature, the growth rate, and the amount of deposited InSb. We have varied these parameters from 365 to  $450^\circ\text{C}$ , from 0.3 to  $1.2 \text{ ML/s}$ , and from 1.8 to 2.6 MLs, respectively. Nevertheless, the InSb QD morphological properties are independent of such variations of the growth conditions, even if very wide. This behavior is in marked contrast to the well known InAs/GaAs system which has, however, a comparable lattice mismatch (6.3% for InSb/GaSb versus 7.1% for InAs/GaAs). This confirms the very long diffusion length of In adatoms on an Sb-terminated surface and shows that no significant improvement in the InSb QDs population can be achieved under usual MBE growth conditions.

To overcome this limitation we have developed an innovative growth procedure with parameters far away from usual MBE conditions. The main key of this technique is the deposition of InSb below the Sb-condensation temperature

followed by an annealing step. After the completion of the GaSb buffer layer we reduce the substrate temperature down to  $\sim 300^\circ\text{C}$ . A few monolayers of InSb are then deposited. The RHEED pattern then becomes very faint. Indeed, at this temperature an amorphous or polycrystalline InSb film is expected. AFM (not shown here) reveals a uniform surface with a root mean square roughness of about 1 ML. Immediately after InSb deposition, the substrate temperature is increased up to the Sb-desorption value ( $390^\circ\text{C}$ ) where an annealing is performed during  $\sim 20\text{--}50 \text{ s}$ . The RHEED pattern evolves toward a spottylike pattern indicating the formation of well developed QDs. Figure 1(b) shows the AFM image (scan size of  $1 \times 1 \mu\text{m}^2$ ) taken from 2.5 ML of InSb deposited according to this procedure. The uniform surface observed after the InSb deposition at low temperature has been replaced by well defined nanostructures after the annealing step. A dot density of  $7.4 \times 10^{10} \text{ cm}^{-2}$ , i.e., one order of magnitude higher than that ever reported, and a narrow monomodal distribution [inset of Fig. 1(b)] are obtained. Their average sizes are strongly reduced down to  $13 \pm 3 \text{ nm}$  for the radius and 1–3 nm for the height. Therefore, this two step growth technique enables a noticeable improvement of the dot distribution, with respect to any other reported conditions. These results are interpreted as follows. At a temperature as low as  $300^\circ\text{C}$ , not only the In-migration length is naturally reduced but also Sb-solid clusters are formed which further suppress In migration. The annealing step allows the evaporation of the excess Sb. The InSb film crystallizes and evolves toward its lowest energy state, i.e., formation of well developed QDs. Each parameter involved in this procedure (amount of deposited material, V/III ratio, heating rate, and annealing time) has its own effect on the final result. For example, a too long annealing step leads to large QDs again.

Plan-view and cross-section TEM analyses have also been performed on such QDs buried within GaSb layers. Figure 2(a) shows a bright-field cross-sectional TEM image (under conditions close to the chemical sensitive 002 two-beam case). It demonstrates the existence of a wetting layer with a high density of QDs by the strong contrast variations along the InSb layer compared to the adjoining homogeneous GaSb. Note that the interfacial zones are free of extended defects, and no threading dislocations are observed in contrast to the previous results for usual MBE growth conditions.<sup>13</sup> By tilting the sample to get the interface inclined to the electron beam and to adjust  $g=220$  diffraction conditions, as shown in Fig. 2(b)), the InSb QDs are clearly detected due to the effect of the strain field on diffracted intensity. The InSb QDs appear to be very uniform, with an average diameter of about 10 nm. The lattice strain field around the InSb QDs appears as lobes of dark contrast (low intensity) with lines of no contrast perpendicular to  $\mathbf{g}$  [the so called coffee bean contrast,<sup>14</sup> more evident in the inset of Fig. 2(b)]. This particular strain effect corresponds to fully strained InSb QDs with an ovoid or almost spherical shape.

Finally, Fig. 3(a) shows PL spectra taken under different excitation intensities at 90 K from this high density InSb/GaSb QD sample. Even under low optical excitation intensity ( $4 \times 10^{-1} \text{ W/cm}^2$ ), the sample exhibits PL emission peaked at 360 meV with a full width at half maximum of 47 meV which we attribute to transitions involving the QD ground state (GS). A second peak is also evident at higher energy (500 meV) and its band filling dynamics at different

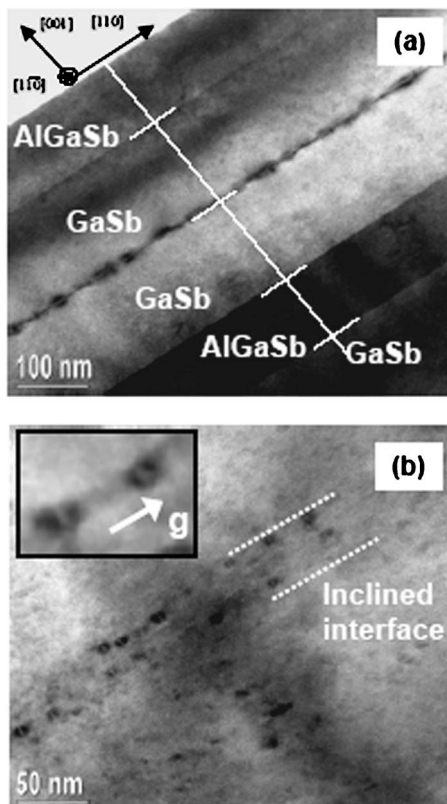


FIG. 2. TEM cross sectional images of 3 ML InSb QDs grown with the two step technique. Cross-sectional 002 bright-field (a) TEM of buried InSb QDs and projectional view (b) of tilted QDs layer ( $g=220$ ) in bright-field mode to visualize the isolated QDs. The inset in (b) is a zoom on two InSb QDs showing the characteristic coffee beam contrast of fully strained nanostructures.

excitation intensities suggests that it is likely due to the first excited state transition in the QDs. The PL peaks related to the QD emission are located at energies lower than previously reported<sup>15</sup> which may be explained taking into account the tensile strain in the GaSb matrix around the QDs. This strain locally lowers the GaSb conduction band thus localizing the electrons and decreasing the transition energy. The other peaks in the 0.7–0.8 eV region are related to GaSb and its native defects,<sup>16</sup> and to the two dimensional InSb wetting layer with a thickness of about 1 ML. This estimate comes from the difference between the total amount of deposited InSb and its amount in InSb QDs evaluated via a statistical analysis of InSb QDs total volume in AFM topography images. The QD emission can be detected up to room temperature [Fig. 3(b)]. The QD GS integrated intensity only decreases by a factor of 4 when the temperature increases from 90 to 300 K, suggesting a good thermal stability.

In conclusion, we have developed a multistep MBE growth procedure for InSb/GaSb QD formation. This technique consists in the deposition of InSb at very low temperature followed by an annealing step. We have obtained the highest density ever achieved ( $>7 \times 10^{10} \text{ cm}^{-2}$ ) of small, fully strained InSb QDs with narrow monomodal size distribution. The QD structures demonstrated PL emission near  $3.5 \mu\text{m}$  up to room temperature.

Part of this work is supported by the European Commission (Project No. FP6-017383, DOMINO).

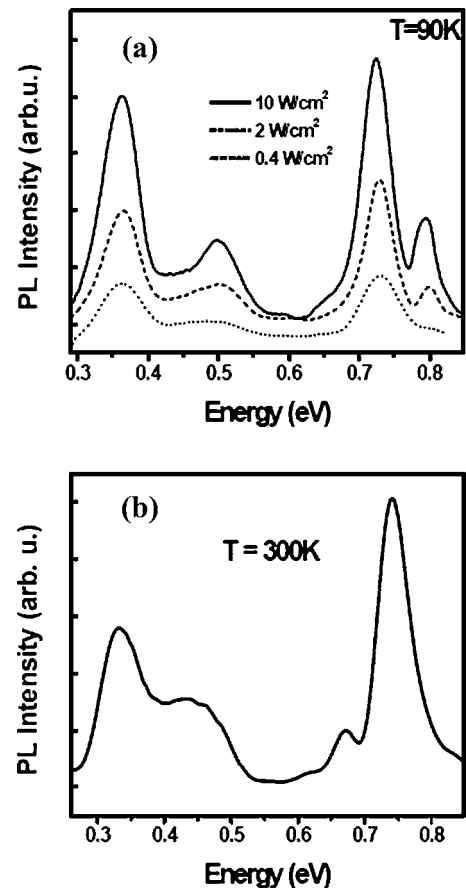


FIG. 3. PL spectra taken from the high density InSb/GaSb QD sample at 90 K (a) under different excitation intensities and at room temperature (b).

- <sup>1</sup>S. J. Smith, G. R. Nash, M. Fearn, L. Buckle, M. T. Emeny, and T. Ashley, *Appl. Phys. Lett.* **88**, 081909 (2006).
- <sup>2</sup>Y. Arakawa and H. Sakaki, *Appl. Phys. Lett.* **40**, 939 (1982).
- <sup>3</sup>B. R. Bennett, B. V. Shanabrook, P. M. Thibado, L. J. Whitman, and R. Magno, *J. Cryst. Growth* **175/176**, 888 (1997).
- <sup>4</sup>S. Shusterman, Y. Paltiel, A. Sher, V. Ezersky, and Y. Rosenwaks, *J. Cryst. Growth* **291**, 363 (2006).
- <sup>5</sup>F. Hatami, S. M. Kim, H. B. Yuen, and J. S. Harris, *Appl. Phys. Lett.* **89**, 133115 (2006).
- <sup>6</sup>N. Bertru, O. Brandt, M. Wassermeier, and K. Ploog, *Appl. Phys. Lett.* **68**, 31 (1996).
- <sup>7</sup>E. Alphandéry, R. J. Nicholas, N. J. Mason, B. Zhang, P. Möck, and G. R. Booker, *Appl. Phys. Lett.* **74**, 2041 (1999).
- <sup>8</sup>Y. Qiu and D. Uhl, *Appl. Phys. Lett.* **84**, 1510 (2004).
- <sup>9</sup>S. V. Ivanov, A. N. Semenov, V. A. Solov'ev, O. G. Lyublinskaya, Ya. V. Terent'ev, B. Ya. Meltser, L. G. Prokopova, A. A. Sitnikova, A. A. Usikova, A. A. Toropov, and P. S. Kop'ev, *J. Cryst. Growth* **278**, 72 (2005).
- <sup>10</sup>V. A. Solov'ev, O. G. Lyublinskaya, A. N. Semenov, B. Ya. Meltser, D. D. Solnyshkov, Ya. V. Terent'ev, L. A. Prokopova, A. A. Toropov, S. V. Ivanov, and P. S. Kop'ev, *Appl. Phys. Lett.* **86**, 011109 (2005).
- <sup>11</sup>N. Deguffroy, M. Ramonda, A. N. Baranov, and E. Tournié, *Proceedings of the 12th International Conference on Narrow-Gap Semiconductors (NGS-12)*, Toulouse 2005, [Inst. Phys. Conf. Ser. **187**, 93 (2006)].
- <sup>12</sup>V. Tasco, N. Deguffroy, A. N. Baranov, E. Tournié, B. Satpati, and A. Trampert, *Phys. Status Solidi B* **243**, 3959 (2006).
- <sup>13</sup>N. Deguffroy, V. Tasco, A. N. Baranov, B. Satpati, A. Trampert, M. Dunaevski, A. Titkov, F. Genty, and E. Tournié, *Phys. Status Solidi C* (to be published).
- <sup>14</sup>D. B. Williams and C. B. Carter, *Transmission Electron Microscopy: A Textbook in Material Science* (Plenum, New York, 1996), Vol. III, p. 417.
- <sup>15</sup>E. Alphandéry, R. J. Nicholas, N. J. Mason, S. G. Lyapun, and P. C. Klipstein, *Phys. Rev. B* **65**, 115322 (2002).
- <sup>16</sup>P. S. Dutta, H. L. Bhat, and Vikram Kumar, *J. Appl. Phys.* **81**, 5821 (1997).